

Synthesis, Characterization, and Antimicrobial Evaluation of a New Bis(semicarbazone) Ligand and Its Coordination Complexes



Mohamad AbdulKarim Hameed¹, Mohamad J. Al-Jeboori^{2*}

²General Directorate of Education for Al-Anbar, Directorate of Heet Education, Anbar, Iraq

¹Department of Chemistry, College of Education for Pure Science (Ibn Al-Haitham), University of Baghdad, Baghdad, Iraq

mohamadal-jeboori@ihcoedu.uobaghdad.edu.iq; mohamadaljeboori@yahoo.com

ARTICLE INFO

Received: 28 / 08 /2024

Accepted: 15/ 10 /2024

Available online: 08/ 06 /2025

DOI: 10.37652/juaps.2024.153186.1314

Keywords:

Bis(semicarbazone) ligand,
Paramagnetic complexes, Synthesis
and characterization, Thermal
stability, Antimicrobial evaluation

ABSTRACT

This study aimed to synthesize a new multidentate bis(semicarbazone) ligand, (2Z,2'E)-2,2'-(((propane-1,3-diylbis(oxy))bis(2,1-phenylene))bis(methanylylidene))-bis(hydrazine-1-carboxamide) (H₂ L), and to investigate its paramagnetic coordination compounds with bivalent transition metals (M(II) = Mn, Fe, Co, Ni, and Cu). It focused on characterizing the ligand and its coordination compounds through physicochemical properties and evaluating their antimicrobial activity. H₂ L was synthesized via a two-step process: First, precursor L was prepared and subsequently reacted with semicarbazide in a 1:2 molar ratio. A range of monomeric paramagnetic coordination compounds was isolated by reacting H₂ L with metal chlorides including manganese(II), iron(II), cobalt(II), nickel(II), and copper(II) in a 1:1 molar ratio. The structures of H₂ L and its complexes were confirmed using various analytical techniques, including FT-IR, UV-Vis spectroscopy, mass spectrometry, NMR spectroscopy, elemental analysis, magnetic moment measurements, and molar conductance measurements. TGA and DTA for H₂ L and selected complexes were also conducted. The antimicrobial activity of H₂ L and its coordination compounds was evaluated against a broad spectrum of bacterial (*Staphylococcus aureus*, *Bacillus subtilis*, *Escherichia coli*, and *Proteus vulgaris*) and fungal (*Candida albicans*) species. The coordination compounds exhibited enhanced antimicrobial activity compared with free H₂ L, with nickel(II) and copper(II) complexes demonstrating the highest activity against bacterial strains, surpassing the efficacy of amoxicillin. In addition, the cobalt(II) and copper(II) complexes showed remarkable inhibition against *C. albicans* compared with the commercial antifungal metronidazole.

Copyright©Authors, 2025, College of Sciences, University of Anbar. This is an open-access article under the CC BY 4.0 license (<http://creativecommons.org/licenses/by/4.0/>).



Introduction

The expansion of chemistry, particularly in coordination chemistry, is largely attributed to the design and synthesis of novel small organic compounds that serve as ligands [1]. Consequently, small organic molecules containing different heteroatoms, acting as donor atoms, have been introduced to develop synthetic chemistry [2-5]. These ligands can impart remarkable electronic properties and steric effects, thereby influencing the metal environment, including its coordination sphere.

The advancements in this area are often related to the development of novel binding systems based on simple, well-designed ligands [6-8]. An example of such ligands is multidentate ligands, including macrocyclic types, which are crucial for stabilizing monomeric and dimeric complexes caused by the chelate effect [9-11]. These compounds (ligands and coordination compounds) have diverse applications in catalysis [1], photovoltaic technologies [12], medicine, and the pharmaceutical field [13,14].

The synthesis of bis-functionalized compounds has received considerable attention from researchers because of their applications in chemistry, biological systems, industry, and material science [2,15,16]. A prominent example of these ligands includes Schiff bases, such as

*Corresponding author at: Department of Chemistry, College of Education for Pure Science (Ibn Al-Haitham), University of Baghdad, Baghdad, Iraq.

ORCID: <https://orcid.org/0000-0002-7050-3944>,

Tel: +964 7826968998

Email: mohamadal-jeboori@ihcoedu.uobaghdad.edu.iq.

semicarbazones, oximes, and their structural analogs, among the most extensively studied ligands in coordination chemistry [9, 11]. Ligands formed from bis-functionalized precursors, including bis-(aldehydes) [9,11,17] or di-(ketones) [18], are notable organic species used in the synthesis of bis(Schiff bases). These bis(Schiff bases) served as complexing agents, facilitating the synthesis of a range of coordination compounds. Furthermore, the formation of bis(aldehydes) compounds with O₄ donor atoms was recently investigated, such as 2,2'-[ethane-1,2-diylbis(oxy)]dibenzaldehyde (EDD) [2], 2,2'-(propane-1,3-diylbis(oxy))dibenzaldehyde (L) [19], and their coordination compounds. These small ligands, featuring two carbonyl groups and two ether oxygen donor atoms, have demonstrated that these donor atoms play a crucial role in complexation. They were utilized to investigate their coordination abilities and biological activities with various metal centers. In addition, these studies investigated the impact of introducing an extra CH₂ group in the spacer of ligand L, in comparison with EDD, on the rigidity of the ligand and its effect on the coordination ability of the oxygen donor atoms toward the metal center, as well as the biological efficacy of the synthesized compounds.

These bis(aldehydes) compounds can serve as precursors forming new bis(Schiff bases), including carbazone ligands. Interestingly, although literature extensively reports the formation of thiosemicarbazone ligands, no reports on the isolation of bis(semicarbazone) ligands, derived from EDD or L, have been found. Therefore, this study aims to explore the formation of a new multidentate bis(semicarbazone) ligand, (2Z,2'E)-2,2'-(((propane-1,3-diylbis(oxy))bis(2,1-phenylene))bis-(methanylylidene))bis(hydrazine-1-carboxamide) (H₂L), which is derived from the reaction of L with semicarbazide. This study also aimed to assess the coordination ability of the two oxygen ether groups, along with the two imine and two carbonyl amide groups, with a range of metal ions. The reaction of the ligand with these metal ions resulted in the isolation of monomeric paramagnetic coordination compounds. Physicochemical techniques were used to characterize the prepared compounds, and thermogravimetric analysis (TGA) and differential thermal analysis (DTA) were conducted to

evaluate their thermal stability. Furthermore, the biological properties of the new H₂L ligand and its subsequent coordination compounds were examined.

Materials and Methods

Commercial reagents, including analytical grade solvents from Sigma-Aldrich, Merck, B.D.H, Alpha chemika, Haymankimia, and CHEM suppliers, were used in this study without any further purification. FTIR spectra were obtained using a Shimadzu FTIR-8400S at the College of Science, University of Baghdad, using KBr or CsI discs in the range of 4000–250 cm⁻¹. Electrospray ionization (+) mass spectroscopy (ESI-MS) of the ligand was conducted using an Agilent Sciex instrument at Mashhad University, Islamic Republic of Iran.

The NMR spectra (¹H and ¹³C) were recorded using a Bruker 400 MHz spectrometer with TMS as an internal standard, and DMSO-d₆ was used as a solvent. The samples were provided by the Department of Chemistry, University of Basrah. The UV-Vis spectra of H₂L and its metal complexes were performed at room temperature using a Shimadzu 1800 spectrometer in a dimethyl sulfoxide solution in the range of 200–1000 nm at the Environmental Laboratory Center, University of Baghdad.

The uncorrected melting points were determined by using Stewart SMP40 at Baghdad University. Elemental analysis was performed by using EuroEA 3000 at Tehran University, Islamic Republic of Iran. Metal and chloride contents of the complexes were determined by using a Shimadzu AA-680G atomic absorption spectrometer, and potentiometric titration was performed by using Metrohm 686 Titro Processor-665 Dosimat. Analyses were conducted at Ibn Sina Company, Baghdad. Magnetic susceptibility measurements were performed at 295 K using a Sherwood Scientific magnetic susceptibility balance at Al-Mustansiriya University, whereas molar conductivities of the complexes were measured by using Cyberscan CON 510 at Baghdad University.

Thermogravimetric analysis and differential thermal analysis were conducted using a STA PT-1000 model instrument from Linseis, Germany. The samples were heated at a rate of 10 °C/min, with the analyses performed at Tehran University, Islamic Republic of Iran.

Synthesis of (2Z,2'E)-2,2'-(((propane-1,3-diyl)bis(oxy))bis(2,1-phenylene))bis(methanylylidene))bis(hydrazine-1-carboxamide)

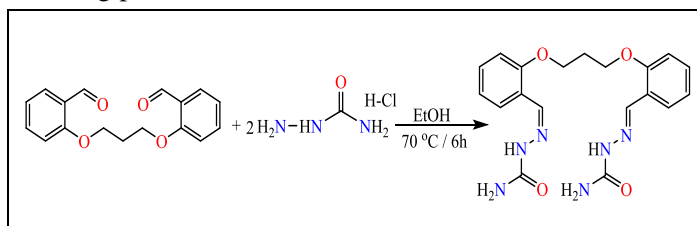
The preparation of H₂ L involved a two-step procedure: first, the synthesis of the bis(aldehyde) compound (L) [2,19], followed by its reaction with semicarbazide as described below.

A solution was prepared by heating and stirring KOH (0.112 g, 2 mmol) and semicarbazide hydrochloride (0.222 g, 2 mmol) in 15 mL of EtOH for 15 min. The mixture was filtered, and the filtrate was slowly introduced into a solution containing 0.3 g (1 mmol) of L dissolved in 15 mL of EtOH. The resulting solution was heated at 70 °C for 6 h. After allowing the reaction to stand at room temperature, a solid was formed, which was then isolated by filtration and washed with 5 mL of ethanol before air drying. The desired semicarbazone ligand product was obtained, yielding 0.323 g of a light-yellow solid (81%), with a melting point of 249–250 °C. ¹H NMR (400 MHz, DMSO-d₆); 10.24 (2H, s, N2,2'-H), 8.24 (2H, s, -N=C_{9,9}-H), 7.98-7.96 (2H, d, C_{7,7}-H, J = 7.6 Hz), 7.32-7.29 (2H, t, C_{5,5}-H, J = 7.4 Hz), 7.08-7.06 (2H, d, C_{4,4}-H, J = 8.32 Hz), 6.96-6.92 (2H, t, C_{6,6}-H, J = 7.48 Hz), 6.45 (4H, b, N(3,3')-H), 4.24-4.21 (4H, t, C_{1,1}-H, J = 5.92; 6.04 Hz), 2.22-2.15 (2H, q, C₂-H, J = 5.96 Hz). In the ¹³C NMR (100 MHz, DMSO-d₆), the resonance assigned to C=O appeared as a single signal at δ_c = 156.76 ppm. A signal related to C_{3,3'} appeared at δ_c = 157.23 ppm. The resonance at 135.42 ppm was linked to the (-C=N-)imine. Resonances correlated with C_{5,5}, C_{7,7}, C_{6,6}, C_{4,4}, and C_{8,8} were observed at 130.82, 126.00, 123.44, 121.12, and 112.92 ppm, respectively. The signal detected at 65.01 ppm was correlated with C_{1,1}. The resonance in the aliphatic region at 29.25 ppm was assigned to C₂ [2,19].

Synthesis of complexes

The complexes were generated using a similar method, and the synthesis of the Mn(II) complex serves as an example: A mixture of H₂L (0.05 g, 0.13 mmol) in 10 mL of 20/80% (v:v) DMF:EtOH was heated, and then a solution containing manganese(II) chloride tetrahydrate (0.025 g, 0.13 mmol), dissolved in 5 mL of ethanol, was added slowly to the clear solution. After stirring the

reaction mixture at 70 °C for 4 h, the solution was cooled to room temperature. A precipitate was formed as the solvent was evaporated. The solid was then washed with diethyl ether. The desired manganese(II) complex was obtained, yielding 0.072 g (64%), with an uncorrected melting point of 246 °C–248 °C.



Scheme 1. Preparation route and reaction conditions of H₂L

Biological efficacy measurements

The prepared compounds (H₂L and its coordination compounds) were assessed for their antimicrobial activity against three bacterial species, namely, *Staphylococcus aureus*, *Escherichia coli*, and *Proteus vulgaris*, and the fungus *Candida albicans*. The agar well diffusion method was used for this evaluation [2,3]. In this technique, sterile metallic borers were used to create wells in the agar media, ensuring a minimum diameter of 6 mm for the well centers. A recommended volume of 100 μL of the test sample solution (1 mg/mL in DMSO) was dispensed into each designated well. Then, the plates were placed in an incubator at 37 °C for 24 h. The antimicrobial effect was determined by measuring the diameter (in mm) of the zones of inhibition around the wells. The activity of the test compounds was compared to reference antibiotics, namely, amoxicillin and metronidazole.

Results and Discussion

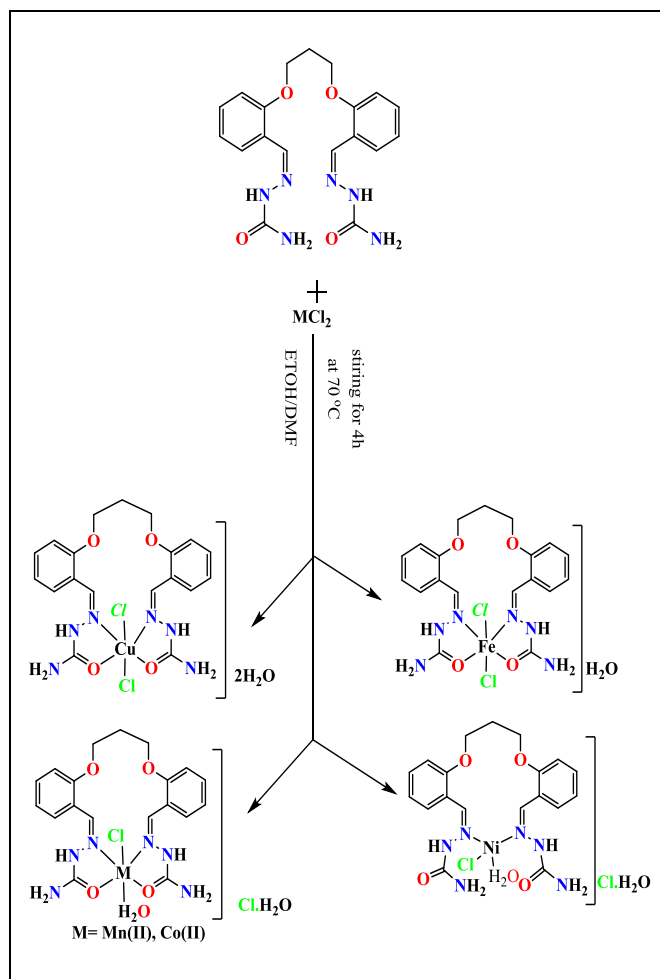
Chemistry

The ligand H₂ L was synthesized in two steps. First, compound L was prepared in accordance with a previously reported method [2,19] by reacting two molecules of salicylaldehyde with 1,3-dibromopropane, after converting salicylaldehyde to potassium 2-formylphenolate using potassium hydroxide in ethanol as a solvent. In the second step, compound L was reacted with an ethanolic solution of semicarbazide hydrochloride in a 1:2 molar ratio (Scheme 1). Compound H₂L was obtained with a substantial yield and examined through a range of physicochemical techniques, including m.p., elemental microanalysis (Table 1), FT-IR (Table 2),

and UV–Vis (Table 3), ESMS, ¹H-, and ¹³C-NMR spectroscopy. A range of coordination compounds was formed upon the interaction of H₂L with Mn(II), Fe(II), Co(II), Ni(II), and Cu(II) ions, which performed in a 1:1 (L:M) molar ratio implementing a solution of EtOH/DMF in 2:8 ratios at reflux (Scheme 2). Furthermore, the complexation is influenced by the solvent and temperature, forming unidentified residues when different solvents or temperatures are used. Spectroscopic and analytical techniques were implemented to characterize the coordination compounds, including elemental microanalysis, metal content, and chloride percentage (Table 1).

Table 1. Characterization of ligand H₂L and its metal complexes: physical and elemental properties

Compound	Color	m.p. °C	Yield %	Micro-analysis; (calculated) and found %						Λ _M S.cm ² .mole ⁻¹
				C	H	N	M	Cl		
H ₂ L	Pale brown	249-250	81	(57.28) 57.36	(5.57) 5.44	(21.09) 21.22	-	-	-	
[Mn(H ₂ L)Cl(H ₂ O)]Cl.H ₂ O (1)	Light brown	246-248	64	(40.71) 40.63	(4.64) 5.11	(15.00) 15.16	(9.82) 9.75	(12.68)	52.8	
[Fe(H ₂ L)Cl ₂].H ₂ O (2)	Brown	248-250	71	(41.99) 42.06	(4.42) 4.86	(15.47) 15.53	(10.31) 10.33	(13.08)	26.2	
[Co(H ₂ L)Cl(H ₂ O)]Cl.H ₂ O (3)	Light blue	254-256	95	(40.43) 40.52	(4.61) 4.75	(14.89) 15.03	(10.46) 10.43	(12.59)	68.5	
[Ni(H ₂ L)Cl(H ₂ O)]Cl.H ₂ O (4)	Light green	166-167	75	(40.43) 40.35	(4.61) 4.88	(14.89) 14.83	(10.46) 10.51	(12.59)	32.5	
[Cu(H ₂ L)Cl ₂].2H ₂ O (5)	Green	159-160	95	(40.07) 39.96	(4.57) 4.82	(14.76) 14.71	(11.25) 11.16	(12.48)	22.4	



Scheme 2. Synthesis route of H₂L coordination compounds

The elemental microanalysis data for ligand (H₂ L) and its metal complexes show good agreement between the calculated and experimental values, confirming the successful synthesis of these compounds. The minor deviation in hydrogen content may be attributed to the presence of coordinated or hydrated water molecules or experimental factors such as moisture absorption during analysis. Such slight discrepancies are common in metal coordination complexes, and they do not compromise the overall consistency and reliability of the results. The main spectroscopic tools cover FT-IR (Table 2) and UV–Vis spectroscopy (Table 3). The conductivity behavior of H₂L complexes in DMSO was investigated by comparing their molar conductance (Λ_M) values with literature data. The Mn(II), Co(II), and Ni(II) coordination complexes exhibited conductance values ranging from 32.5 to 68.5 S.cm².mol⁻¹, indicating 1:1 electrolyte behavior in DMSO [20]. By contrast, the Fe(II) and Cu(II) complexes

exhibited conductivity values of 26.2 and 22.4 S.cm².mol⁻¹, respectively, indicating a non-electrolyte behavior (Table 1). The collected spectroscopic and analytical data revealed the isolation of the required ligand H₂L and its coordination compounds.

Spectroscopic characterization

FTIR data

The FT-IR spectrum of H₂L was analyzed (Fig. 1). A peak recorded at 1780 cm⁻¹ is attributed to $\nu(\text{C}=\text{O})$ of the amide group, while the two peaks at 1678 and 1658 cm⁻¹ are attributed to the aldehyde carbonyls in (L). The presence of one peak for the carbonyl of the amide groups indicated that the two moieties are equivalents. The $\nu(\text{C}=\text{N})$ imine stretch is not directly observed as a distinct peak because it is obscured by overlapping absorption with the amide $\nu(\text{C}=\text{O})$ stretch. This overlap shows up as a broad hump around 1660 cm⁻¹ rather than two distinct peaks.

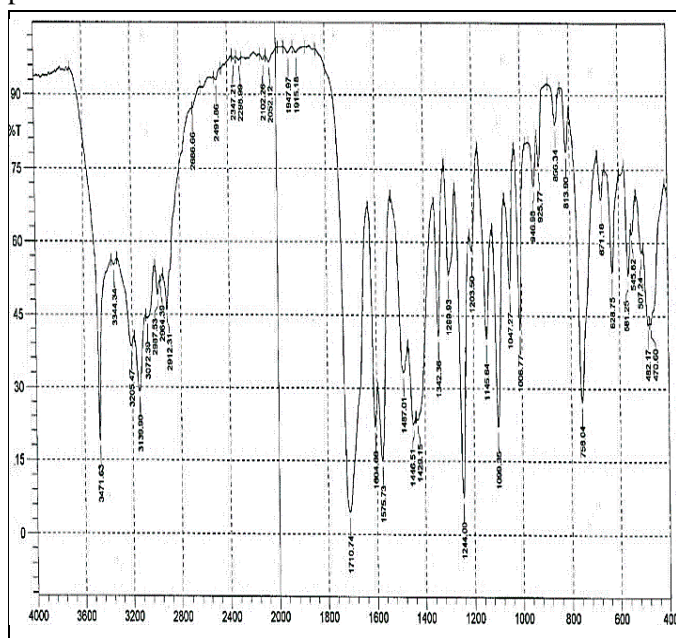


Figure 1. FT-IR spectrum of H₂L

The spectra of the complexes indicated a shift in the value of the $\nu(\text{C}=\text{O})$ amide carbonyl group. The $\nu(\text{C}=\text{O})$ amide carbonyl group in complexes 1, 2, 3, and 4 was detected at a higher wavenumber, and it appeared at 1712 cm⁻¹, which is contrary to that in the H₂L compound at 1710 cm⁻¹. However, complex 5 revealed a shift to a lower frequency at 1708 cm⁻¹. The shift in the $\nu(\text{C}=\text{O})$ amide carbonyl group may indicate the involvement of

the $\nu(\text{C}=\text{O})$ carbonyl moiety in coordination with the metal ion [2,19]. The oxygen-ether $\nu(\text{C}-\text{O}-\text{C})$ band detected at 1244 cm⁻¹ in the free ligand did not show any change in wavelength for all complexes, indicating that this part is not bound in coordination with the transition metals. The spectra of the complexes revealed a distinct peak at 1664–1674 cm⁻¹ associated with the $\nu(\text{C}=\text{N})$ imine. This peak appeared as a shoulder in the FTIR of the free compound H₂L at ca. 1660 cm⁻¹, overlapping with the $\nu(\text{C}=\text{O})$ amide. The appearance of this band upon complexation may result from the participation of nitrogen atoms in the azomethine group $\nu(\text{C}=\text{N})$ coordinating with the metal ion [3-6]. The spectra of the coordination compounds demonstrated the presence of the $\nu(\text{N}-\text{H})$ hydrazinic group, with a small shift. This finding may confirm the participation of the C=N imine functionality in the complexation, with the ligand acting as a neutral species upon complexation. The FTIR data of the coordination compounds showed supplementary peaks within the range of 600–200 cm⁻¹, which were absent in the H₂L spectrum. The FT-IR spectra detected peaks correlated with $\nu(\text{Mn}-\text{N})$, $\nu(\text{Fe}-\text{N})$, $\nu(\text{Co}-\text{N})$, $\nu(\text{Ni}-\text{N})$, and $\nu(\text{Cu}-\text{N})$ at 484, 472, 487, 476, and 457 cm⁻¹, respectively [3,17,21]. The bands corresponding to $\nu(\text{M}-\text{O})$ carbonyl stretches were identified at 563 cm⁻¹ for $\nu(\text{Mn}-\text{O})$, 549 cm⁻¹ for $\nu(\text{Fe}-\text{O})$, 559 cm⁻¹ for $\nu(\text{Co}-\text{O})$, and 541 cm⁻¹ for $\nu(\text{Cu}-\text{O})$ [2,3,21]. In addition, the bands corresponding to $\nu(\text{M}-\text{Cl})$ stretching were observed at 258, 256;287, 258, 244, and 227;217 cm⁻¹ for the $\nu(\text{Mn}-\text{Cl})$, $\nu(\text{Fe}-\text{Cl})$, $\nu(\text{Co}-\text{Cl})$, $\nu(\text{Ni}-\text{Cl})$, and $\nu(\text{Cu}-\text{Cl})$, respectively [2,3]. Bands related to $\nu(\text{Mn}-\text{OH}_2)$, $\nu(\text{Co}-\text{OH}_2)$, and $\nu(\text{Ni}-\text{OH}_2)$ were detected at 673, 665, and 628 cm⁻¹, respectively [2,3].

NMR and mass spectral data of H₂L

The interpretation of peak positions relies on the atom numbering scheme presented in Fig. 2. The ¹H-NMR of the bis(semicarbazone) conducted in DMSO-d₆ solvent is illustrated in Fig. 3. The spectrum correctly recorded resonances corresponding to the protons of the synthesized ligand. A peak resonated at 10.24 ppm, integrating two protons, is attributed to the hydrazinic group (2H, s, N_{2,2'}-H) [3,6,8].

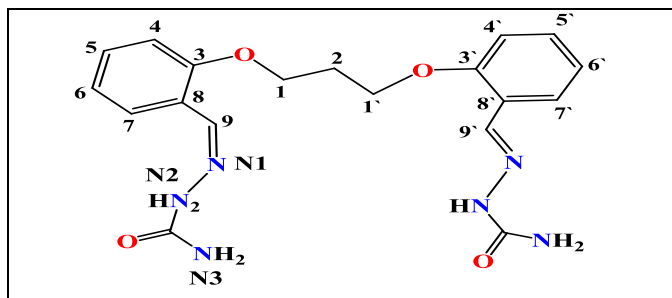


Figure 2. Numbering fashion for the assignment of peaks in the NMR analysis of H₂L

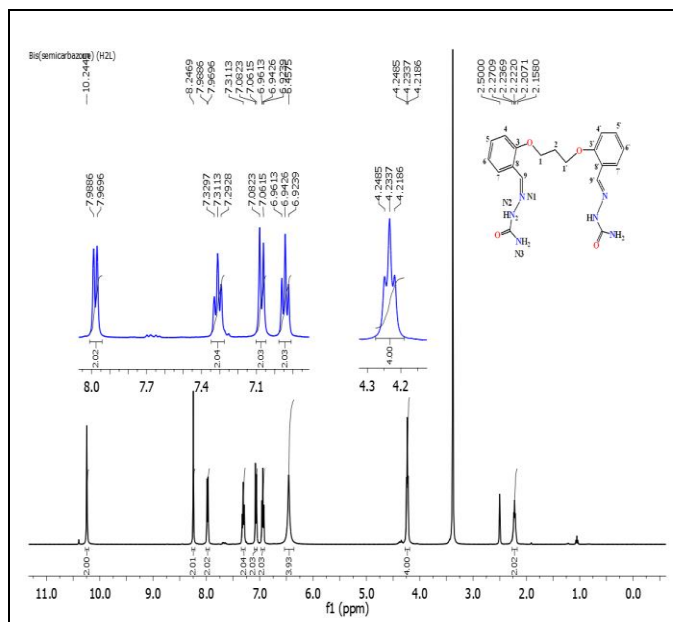


Figure 3. Proton NMR spectrum of H₂L in DMSO-d₆ solvent

The downfield shift of this peak may result from intramolecular hydrogen bonding or intermolecular hydrogen bonding, as observed in the NMR solution. Another peak recorded at 8.24 ppm is attributed to C-H of the imine moiety (2H, s, -N=C_{9,9'}-H), which integrates two protons. In addition, a doublet at 7.98–7.96 ppm, equal to two protons, is linked to (2H, d, C_{7,7'}-H, J = 7.6 Hz). Similarly, a triplet recorded at 7.32–7.29 ppm, integrating two protons, is attributed to (2H, t, C_{5,5'}-H, J = 7.4 Hz). Moreover, a doublet with two protons integrated at 7.08–7.06 ppm is correlated with (2H, d, C_{4,4'}-H, J = 8.32 Hz). Furthermore, a triplet detected at 6.96–6.92 ppm, integrating two protons, is assigned to (2H, d, C_{6,6'}-H, J=7.48 Hz). The broad peak, which integrates four protons, at 6.45 ppm is assigned to the amine group (4H, b, N_{3,3'}-H). Another triplet observed at 4.24–4.21 ppm, equivalent to four protons, is related to

(4H, t, C_{1,1'}-H, J = 5.92; 6.04 Hz). Finally, the quintet peak, integrating two protons, at 2.22–2.15 ppm is attributed to (2H, q, C₂-H, J = 5.96 Hz) [2,19].

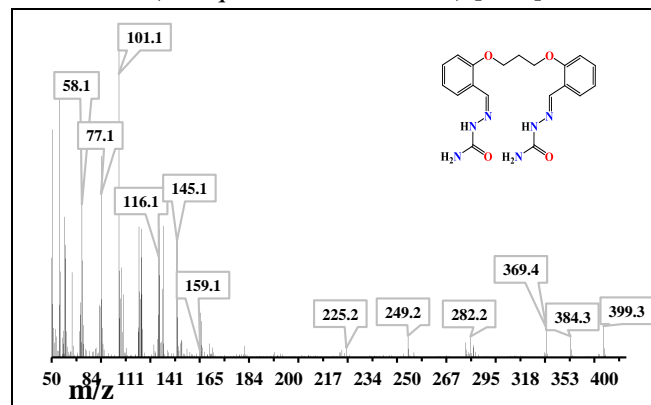


Figure 5. Electrospray (+) mass spectrum of H₂L.

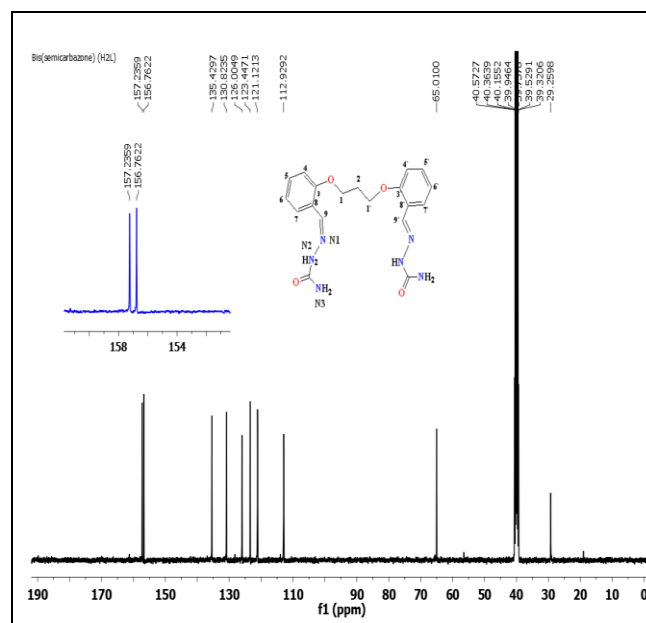


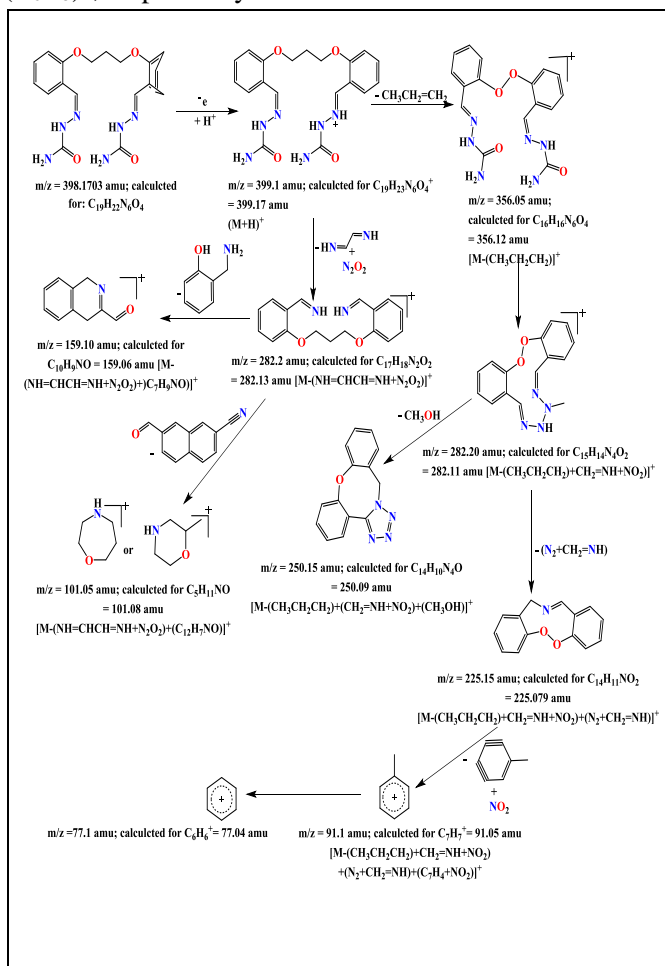
Figure 4. C-13 NMR spectrum of H₂L in DMSO-d₆ solvent

The ¹³C NMR spectrum of H₂L, obtained in DMSO-d₆ solvent, is depicted in Fig. 4. The signals observed at δ_c = 157.23 and 156.76 ppm correspond to (C_{3,3'}) and (C=O) of the semicarbazone moiety, respectively. In addition, the resonance at 135.42 ppm is associated with the (-C=N-)imine C_{4,4'} and C_{8,8'}. The chemical shifts observed at 130.82, 126.00, 123.44, 121.12, and 112.92 ppm are attributed to C_{5,5'}, C_{7,7'}, C_{6,6'}, C_{4,4'}, and C_{8,8'}, respectively.

Furthermore, a resonance at 65.01 ppm is assigned to C_{1,1'}, and a peak at 29.25 ppm is attributed to C₂ [2,19]. Finally, the small peaks observed at 161.05, 137.65, 127.91, 114.08, 56.50, and 18.87 ppm correspond to

another isomer detected in the solution on the NMR time scale.

The electrospray ionization positive mode of H₂L (Fig. 5) exhibits a peak at 399.1 amu. This peak is attributed to the parent ion peak (M)⁺ with a relative intensity of 9.68% (referring to the base ion peak). Furthermore, the base ion peak is recorded at 101.05 amu (100%), which may be ascribed to 1,4-oxazepane or 2-methylmorpholine ions. In addition, the spectrum indicates peaks at 356.05(0.76%), 282.2(8.33%), 225.15(3.41%), 250.09(3.03%), 91.1(61.29%), and 77.1 (59.68%) amu, which are assigned to [M-(CH₃CH₂CH₂)]⁺, [M-(NH=CHCH=NH+N₂O₂)]⁺, [M-(CH₃CH₂CH₂)+CH₂=NH+NO₂]⁺, [M-(CH₃CH₂CH₂)+CH₂=NH+NO₂)+(N₂+CH₂=NH)]⁺, [M-(CH₃CH₂CH₂)+(CH₂=NH+NO₂)+(CH₃OH)]⁺, [M-(CH₃CH₂CH₂)+CH₂=NH+NO₂)+(N₂+CH₂=N+(C₇H₄+NO₂)]⁺, and (C₆H₅)⁺, respectively.



Scheme 3. Suggested fragmentation pattern of H₂L

The successive fragmentation pattern and their proposed assignment are illustrated in Scheme 3.

Electronic spectra and magnetic measurements of coordination compounds

Table 3. Spectroscopic and magnetic data of H₂L and its complexes (with assignments).

Comp.	λ_{nm}	μ_{eff}	ϵ_{max} ($dm^3 \cdot mol^{-1} \cdot cm^{-1}$)	Assignment	10Dq (cm^{-1})
H ₂ L	256 291 320		2038 1428 1445	$\pi \rightarrow \pi^*$ $n \rightarrow \pi^*$ C.T	-
1	256 292 322 891 988	5.58	2038 1409 1445 5 9	L.F L.F C.T ${}^6A_{1g} \rightarrow {}^4T_{1g}^{(P)}$ ${}^6A_{1g} \rightarrow {}^4T_{1g}^{(G)}$	10121
2	291 318 915 983	4.95	492 301 52 52	L.F C.T ${}^6A_{1g} \rightarrow {}^6E_{1g}$ ${}^6A_{1g} \rightarrow {}^6E_{1g}$	11303
3	293 321 532 667 992	4.27	2314 2512 23 17 6	L.F C.T ${}^4T_{1g}^{(F)} \rightarrow {}^4T_{1g}^{(P)}$ ${}^4T_{1g}^{(F)} \rightarrow {}^4A_{2g}^{(F)}$ ${}^4T_{1g}^{(F)} \rightarrow {}^4T_{2g}^{(F)}$	12601
4	252 292 318 888 990	3.54	1870 1385 1380 6 7	L.F L.F C.T ${}^3T_{1g}^{(F)} \rightarrow {}^3T_{1g}^{(P)}$ ${}^3T_{1g}^{(F)} \rightarrow {}^3A_{2g}^{(F)}$	10101
5	291 318 823 915 982	2.07	735 672 54 5 47	L.F C.T ${}^2B_{1g} \rightarrow {}^2A_{2g}$ ${}^2B_{1g} \rightarrow {}^2B_{2g}$ ${}^2B_{1g} \rightarrow {}^2E_g$	10183

The electronic spectra of H₂L and its coordination compounds were measured in DMSO solutions at a concentration of 10⁻³ M (Table 3). The UV–Vis spectrum of H₂L reveals three peaks at 256, 291, and 320 nm because of the field effect of the ligands $\pi \rightarrow \pi^*$, $n \rightarrow \pi^*$, and C.T., respectively [1,2,8]. The spectra of the metal complexes display peaks around 252–292 and 318–322 nm. These peaks are attributed to ligand field (L.F.; $\pi \rightarrow \pi^*$ and $n \rightarrow \pi^*$) and charge transfer (C.T.) transitions, respectively [22-24]. The Mn(II) complex reveals peaks at 891 and 988 nm, which are linked to ${}^6A_{1g} \rightarrow {}^4T_{1g}^{(P)}$ and ${}^6A_{1g} \rightarrow {}^4T_{1g}^{(G)}$, respectively, indicating a distorted octahedral geometry about the Mn(II) core [23,25]. This

observation follows the high-spin d^5 configuration for Mn(II), as supported by the magnetic moment value of

5.58 BM. The peaks observed at 915 and 983 nm in the Fe(II) spectrum, corresponding to the transitions ${}^6A_{1g} \rightarrow {}^6E_{1g}^{(G)}$ and ${}^6A_{1g} \rightarrow {}^6E_{1g}$, respectively, confirm the distorted octahedral coordination arrangement surrounding the metal center, as supported by the magnetic moment value of 4.95 BM [2]. The peaks observed at 532, 667, and 992 nm in the Co(II) spectrum correspond to the transitions ${}^4T_{1g}^{(F)} \rightarrow {}^4T_{1g}^{(P)}$, ${}^4T_{1g}^{(F)} \rightarrow {}^4A_{2g}^{(F)}$, and ${}^4T_{1g}^{(F)} \rightarrow {}^4T_{2g}^{(F)}$, respectively. These transitions provide experimental evidence confirming a distorted octahedral coordination arrangement about the central cobalt ion [3]. This finding is supported by the high-spin d^7 configuration of Co(II) (magnetic moment = 4.27 BM) with three unpaired electrons. In the Ni(II) complex, the bands observed at 888 and 990 nm are attributed to the transitions ${}^3T_{1g}^{(F)} \rightarrow {}^3T_{1g}^{(P)}$ and ${}^3T_{1g}^{(F)} \rightarrow {}^3A_{2g}^{(F)}$, respectively. These spectral features provide evidence supporting the presence of a distorted tetrahedral coordination geometry around the central nickel ion [26]. Finally, the peaks observed at 460, 468, and 478 nm in the Cu(II) spectrum correspond to the transitions ${}^2B_{1g} \rightarrow {}^2A_{2g}$, ${}^2B_{1g} \rightarrow {}^2B_{2g}$, and ${}^2B_{1g} \rightarrow {}^2E_g$, respectively. The magnetic moment value of 1.84 BM for the Cu(II) coordination compound is within the expected range for the d^9 configuration with one unpaired electron observed previously for distorted octahedral geometries [24,27]. The calculated $10Dq$ values for the Mn(II), Fe(II), Co(II), and Cu(II) complexes, all of which adopt distorted octahedral geometries, are consistent with the typical range reported in the literature for high-spin, octahedral complexes with weak-to-moderate ligand fields [28,29]. By contrast, the calculated $10Dq$ value of 10101 cm^{-1} for the tetrahedral Ni(II) complex is slightly higher than the values typically observed for tetrahedral Ni(II) complexes. Although the ligand generally behaves as a weak field, forming high-spin octahedral complexes, the Ni(II) complex may indicate a stronger-than-expected ligand field probably because of the number of covalent interactions or distortions that enhance the crystal field [28,29].

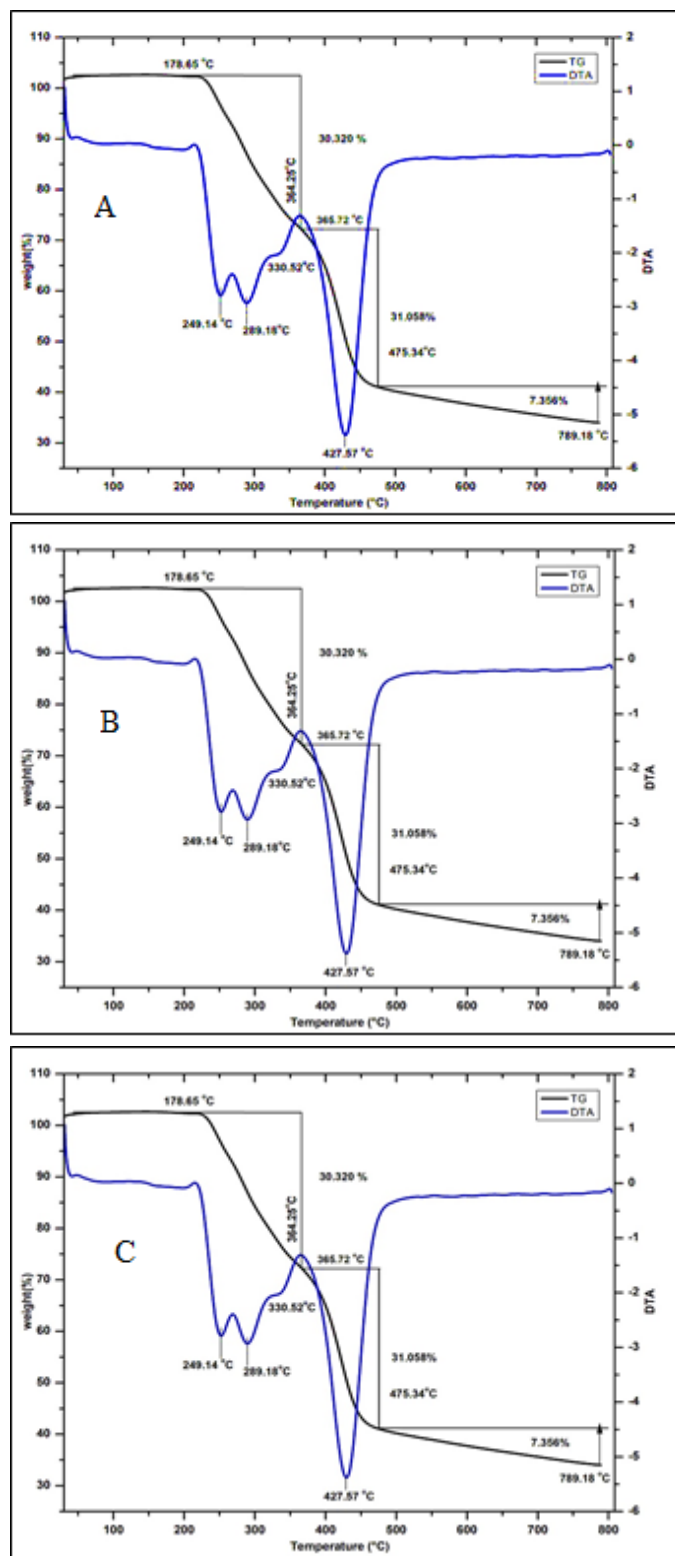


Figure 4. TGA and DTA thermograms of (A) H_2L , (B) Ni(II) complex, and (C) Cu(II) complex

TGA and DTA

Thermal decomposition of H_2L

The thermal analysis thermograms (TGA and DTA) of H_2L are depicted in Fig. 4A. The TGA data

indicate that the ligand undergoes thermal decomposition in three distinct steps. As shown in the DTA thermogram, the first step includes three decomposition processes. This step, which was observed between 178.65 ° C and 365.72 ° C, is attributed to the mass loss of C₆H₇N and HCN, showing a weight loss of 30.320% (theo. 30.138%), The dissociation step, which was recorded from 365.72 ° C to 475.34 ° C, may indicate the mass loss of C₃H₅N, CO, and NH₃ molecules with a weight loss of 31.058% (theo. 31.143%). The peak observed between 475.34 ° C and 789.18 ° C may indicate a loss of NO molecules, which reveals a weight loss of 7.356% (theo. 7.534%). The residue weight observed at 789.18 ° C shows a weight loss of 31.266% (theo. 31.143%), which may indicate the elimination of NO₂ and C₆H₆ molecules. Furthermore, DTA showed an endothermic peak at 249.14 ° C, which is correlated with the melting point of H₂L.

Thermal decomposition of [Ni(H₂L)Cl(H₂O)]Cl.H₂O

The thermal analysis thermograms (TGA and DTA) of [Ni(H₂L)ClH₂O]Cl.H₂O are shown in Fig. 4B. The TGA and DTA data indicate that the thermal decomposition of the complex takes place in seven steps. The first peak, which is characterized as endothermic in DTA positioned at 80.39 ° C, may be related to the removal of the water hydrate molecule (H₂O). This peak showed 3.258% weight loss (theo. 3.193%). The second step in TGA, which is observed between 125.06 ° C and 226.68 ° C, is attributed to the loss of the aqua water molecule (H₂O), showing 3.446% weight loss (theo. 3.193%). The third step between 226.68 ° C and 261.80 ° C is related to the loss of the HCl fragment, exhibiting 6.475% weight loss (theo. 6.475%). The fourth step, which is recorded between 261.80 ° C and 312.50 ° C, indicated the loss of CO, NH₃, and HCOH, showing 13.565% weight loss (theo. 13.305%). The fifth step, which is observed between 312.50 ° C and 383.05 ° C, indicated the loss of HCONH₂, H₂, and HCl, exhibiting 14.773% weight loss (theo. 14.813%). The sixth step, which is recorded between 383.05 ° C and 466.12 ° C, indicated the loss of C₆H₅Cl and 2HCN, showing 29.545% weight loss (theo. 29.537%). The seventh step, which is recorded between 466.12 ° C and 788.44 ° C,

was designated for the loss of the N₂H₄, revealing 5.860% weight loss (theo. 5.677%). The residue weight observed at 788.44 ° C shows a 23.078% loss in weight (theo. 23.794%), representing the remaining organometallic residue. The DTA chart showed an endothermic peak at 166.21 ° C, which correlates with the degree of dissociation of [Ni(H₂L)ClH₂O]Cl.H₂O.

Thermal analyses of [Cu(H₂L)Cl₂].2H₂O

The thermal examination curves of [Cu(H₂L)Cl₂].2H₂O are depicted in Fig. 4C. The TGA data revealed that the decomposition of the complex takes place in three steps. The first peak, which is noted as endothermic between 39.12 ° C and 167.10 ° C in DTA, is an overlapped peak with more than one process. This peak may be correlated with the removal of the hydrate water molecule (2H₂O), as well as the decomposition point. This step showed a weight loss of 6.428% (theo. 6.332%). The second step, which is recorded between 168.47 ° C and 377.55 ° C, indicates the removal of CO, CO₂, C₂H₂, C₆H₆, and 2HCl molecules, revealing a weight loss of 43.856% (theo. 43.796%). The third step, which is observed between 377.55 ° C and 789.18 ° C, is related to the loss of 2NH₃, HCN, 2H₂, and N₂H₄ fragments, exhibiting a weight loss of 17.098% (theo. 17.061%). The residue weight observed at 789.18 ° C shows a weight loss of 32.618% (theo. 32.811%), representing the remaining organometallic residue. The degree of decomposition of [Cu(H₂L)Cl₂].2H₂O is observed at 159.32 ° C, which overlapped with the first endothermic peak.

Biological evaluation

The antimicrobial activity of the ligand (H₂L) and its coordination compounds with Mn(II), Fe(II), Co(II), Ni(II), and Cu(II) ions was evaluated against a range of bacterial strains, including *S. aureus*, *Bacillus subtilis*, *E. coli*, and *P. vulgaris*. Separate tests using DMSO solutions were conducted to elucidate the action of DMSO in the biological assessment. Amoxicillin, a well-established antibiotic, served as a reference for antibacterial activity in this study. The findings can be outlined as follows:

- 1- The enhanced activity of the metal complexes may be attributed to their coordination sphere, which influences the conductivity of the complexes.

- 2- Among the tested metal complexes, Cu(II) and Ni(II) demonstrated the highest antibacterial efficacy against the bacterial strains. By contrast, the manganese and iron complexes showed the lowest activity.

Table 4. Evaluation of the inhibitory effect (Mm) of the synthesized metal complexes with ligand H₂L on bacterial and fungal strains

Compound	Bacterial strain					Fungi
	<i>Staphylococcus aureus</i>	<i>Bacillus subtilis</i>	<i>E. coli</i>	<i>Proteus vulgaris</i>	<i>Candida albicans</i>	
Amoxicillin	8	11	9	10	-	
Metronidazole	-	-	-	-	9	
H ₂ L	9	9	9	9	15	
[Mn(H ₂ L)Cl(H ₂ O)]Cl.H ₂ O	12	16	9	9	17	
[Fe(H ₂ L)Cl ₂].H ₂ O	10	9	10	10	17	
[Co(H ₂ L)Cl(H ₂ O)]Cl.H ₂ O	15	18	16	13	23	
[Ni(H ₂ L)Cl(H ₂ O)]Cl.H ₂ O	24	31	28	31	18	
[Cu(H ₂ L)Cl ₂].2H ₂ O	26	25	26	20	26	

- 3- The Cu(II) complex exhibited superior activity compared with the other six-coordinate complexes, which may be due to its d⁹ electron configuration and the formation of a neutral complex. The Ni(II) complex also demonstrated a notable activity, which may be due to its four-coordinate configuration.
- 4- The collected data indicate that the synthesized coordination compounds have excellent antibacterial properties compared with amoxicillin, particularly the Ni(II) and Cu(II) complexes.
- 5- The [Cu(H₂L)Cl₂].2H₂O complex shows high antibacterial activity against all bacterial strains, whereas the [Ni(H₂L)Cl(H₂O)]Cl.H₂O complex exhibits high activity against *B. subtilis*, *E. coli*, and *P. vulgaris*.

The antifungal efficacy of H₂L and its coordination compounds against *C. albicans* was explored. The efficacy of these compounds was compared with metronidazole, which is a standard antifungal drug. The experimental data indicated that the drug metronidazole exhibits a moderate antifungal effect against *C. albicans*, with a 9 mm inhibition zone. By contrast, the ligand demonstrated enhanced activity, showing a 15 mm

inhibition zone, compared with the commercial drug (Table 4). The enhanced activity of the bis(semicarbazone) ligand, compared with the commercial drug, may be attributed to its chemical structure. This ligand contains two semicarbazone moieties (a functional group with the structure (-NH-C=O-NH-N=C-)). By contrast, metronidazole contains a nitro group (-NO₂) attached to an imidazole ring. The ability of the bis(semicarbazone) ligand to disrupt enzyme function and interfere with DNA processes makes it more effective against certain pathogens.

The metal ions markedly enhanced the antifungal behavior of H₂L in complexes. The Cu(II) complex showed the most excellent results with an inhibition zone of 26 mm, indicating strong antifungal activity. The Co(II) complex also showed excellent antifungal activity with an inhibition zone of 23 mm. These results indicate that complexation with specific metals such as cobalt, nickel, and copper greatly enhances antifungal activity.

Conclusions

This study reports the synthesis of a bis(semicarbazone) ligand and five paramagnetic coordination complexes with Mn(II), Fe(II), Co(II), Ni(II), and Cu(II) ions. The ligand (H₂L) was synthesized via the condensation of bis(aldehyde) L with semicarbazide. Physicochemical characterization techniques, including NMR, FTIR, and electronic analyses, were used to validate the structures of H₂L and its coordination complexes. NMR analysis confirmed the presence of the main functional groups, such as hydrazinic, imine, aromatic, and amine groups, and indicated the possibility of isomerism. In particular, the ¹H NMR peak at 10.24 ppm confirms the presence of hydrazinic protons, indicating a downfield shift caused by hydrogen bonding. Similarly, the ¹³C NMR signal at 157.23 ppm confirms the presence of the C=O group in the semicarbazone moiety, which is critical for the ligand's structure. FTIR analysis revealed a ν(C=O) amide peak at 1780 cm⁻¹, with a shift to 1712 cm⁻¹ in the complexes, indicating metal coordination. A distorted tetrahedral geometry was confirmed for the monomeric Ni(II) complex, whereas a distorted octahedral arrangement was proposed for the other complexes. Electronic spectral analysis, together with magnetic

susceptibility values, indicated that the ligand exhibits transitions typical of $\pi \rightarrow \pi^*$, $n \rightarrow \pi^*$, and charge transfer processes. The coordination complexes displayed distinct d-d absorption features, thereby confirming their geometries: The Mn(II), Fe(II), Co(II), and Cu(II) complexes adopt distorted octahedral arrangements, whereas the Ni(II) complex shows a distorted tetrahedral geometry. Furthermore, the $10Dq$ values for the Mn(II), Fe(II), Co(II), and Cu(II) complexes indicate high-spin distorted octahedral geometries, which are characterized by weak ligand fields. By contrast, the $10Dq$ value for the Ni(II) complex indicates a distorted tetrahedral geometry. In addition, TGA and DTA were conducted to assess the thermal stability of the compounds. Antimicrobial activity tests revealed that the coordination complexes were more effective than the free ligand, outperforming commercial antibiotics such as amoxicillin and antifungal drugs such as metronidazole.

Acknowledgements

We gratefully acknowledge the support of the University of Baghdad and the Department of Chemistry, College of Education for Pure Science (Ibn Al-Haitham), for providing a PhD scholarship and laboratory facilities to Mr. MAH.

Conflict of Interest

The authors declare no conflict of interest.

References

- [1] Stradiotto, M., and Lundgren, R.J. *Ligand Design in Metal Chemistry: Reactivity and Catalysis* (John Wiley & Sons, Ltd., 2016). DOI: 10.1002/9781118839621.
- [2] Abaas, D. J., & Al-Jeboori, M. J. (2023). Coordination compounds of carbonyl oxygen polychelate ligand; synthesis, physicochemical characterization and biological evaluation. *Revista Bionatura*, 8(2), 18.
- [3] Abaas, H. J., & Al-Jeboori, M. J. (2023). New dimeric complexes with semicarbazone Mannich-based ligand; formation, structural investigation and biological activity. *Revista Bionatura*, 8(2), 15.
- [4] Al-Rubaye, B. K., Al-Jeboori, M. J., & Potgieter, H. (2021). Metal complexes of multidentate N_2S_2 heterocyclic Schiff-base ligands; formation, structural characterisation and biological activity. *Journal of Physics: Conference Series*, 1879, 022074, 3-20.
- [5] Al-Rubaye, B. K., Hussien, N. J., Abul Rahman, A. S. A. K., Yousif, E. I., & Al-Jeboori, M. J. (2020). New organotin (IV) complexes derived from 3,4-dihydroxybenzaldehyde N(4)-ethyl-3-semicarbazone ligand; synthesis, characterisation and biological activity. *Biochemical and Cellular Archives*, 20(2), 6571-6579.
- [6] Mawat, T. H., & Al-Jeboori, M. J. (2020). Synthesis, characterisation, thermal properties and biological activity of coordination compounds of novel selenosemicarbazone ligands. *Journal of Molecular Structure*, 1208, 127867. <https://doi.org/10.1016/j.molstruc.2020.127876>
- [7] Mawat, T. H., & Al-Jeboori, M. J. (2019). Synthesis and spectral characterisation of new β -aminoketone compounds. *Biochemical and Cellular Archives*, 19(2), 4573-4580.
- [8] Khaleel, H. I., & Al-Rubaye, B. K. (2022). New metal complexes derived from heterocyclic Schiff-base ligand: Preparation, structural investigation and biological activity. *International Journal of Drug Delivery Technology*, 12(03), 1341-1346.
- [9] Al-Jeboori, F. H. A., Hammud, K. K., & Al-Jeboori, M. J. (2014). Synthesis and characterization of new acyclic octadentate ligand and its complexes. *Iranian Journal for Science & Technology*, 38A(4), 489-497.
- [10] Ahmed, R. M., Yousif, E. I., & Al-Jeboori, M. J. (2013). Co(II) and Cd(II) complexes derived from heterocyclic Schiff-bases: Synthesis, structural characterisation, and biological activity. *The Scientific World Journal: Inorganic Chemistry*, 2013, Article ID 754868, 6 pages.
- [11] Issa, I. O., Al-Jeboori, M. J., & Al-Dulaimi, J. S. (2011). Formation of binuclear metal complexes with multidentate Schiff-base oxime ligand: Synthesis and spectral investigation. *Ibn AL-Haitham Journal for Pure and Applied Science*, 24(2), 142-153.
- [12] Conradie, J., Conradie, M. M., Tawfiq, K., Al-Jeboori, M. J., Coles, S. J., Wilson, C., & Potgieter, H. J. (2018). Novel dichloro(bis{2-[1-(4-methyl-

- phenyl)-1H-1,2,3-triazol-4-yl- κN_3] - pyridine- κN)metal(II) coordination compounds of seven transition metals (Mn, Fe, Co, Ni, Cu, Zn and Cd). *Polyhedron*, 151, 243–254.
- [13] Jurca, T., Marian, E., Vicaş, L. G., Mureşan, M. E., & Fritea, L. (2017). Metal Complexes of Pharmaceutical Substances. In *Spectroscopic Analyses Developments and Applications*. InTech. [Online]. Available: <http://dx.doi.org/10.5772/65390>.
- [14] Griffiths, D. V., Al-Jeboori, M. J., Arnold, P. J., Cheong, Y.-K., Duncanson, P., & Motevalli, M. (2010). Studies of rheniumtricarbonyl complexes of tripodal pyridyl-based ligands. *Inorganica Chimica Acta*, 363, 1186-1194.
- [15] Al-Rubaye, B. K., Brink, A., Miller, G. J., Potgieter, H., & Al-Jeboori, M. J. (2017). Crystal structure of (E)-4-benzylidene-6-phenyl-1,2,3,4,7,8,9,10-octahydrophenanthridine. *Acta Crystallographica Section E: Structure Reports Online*, 73, 1092-1096.
- [16] Ali, A., & Merza, J. (2017). Synthesis and characterization of novel dialdehydes based on $\text{S}_{\text{N}}2$ reaction of aromatic aldehyde. *Inorganic Chemistry and Industrial Journal*, 2, 111-119.
- [17] Zayed, E. M., Zayed, M. A., Fahim, A. M., & El-Samahy, F. A. (2017). Synthesis of novel macrocyclic Schiff's- base and its complexes having N_2O_2 group of donor atoms: Characterization and anticancer screening. *Applied Organometallic Chemistry*, 31(9), 1-7.
- [18] Al-Jeboori, M. J., Abdulkarim, E. I., & Attia, S. (2015). Synthesis and characterization of novel ligand type N_2O_2 and its complexes with Cu(II), Co(II), Ni(II), Zn(II), and Cd(II) ions. *Ibn AL-Haitham Journal for Pure and Applied Science*, 18(2), 51-67.
- [19] Hameed, M. A., & Al-Jeboori, M. J. (2024). Synthesis, structural characterisation, and biological activity of new coordination compounds with polychelate ligand incorporating carbonyl and ether oxygen sites. Paper accepted for presentation at *The Second Samarra International Conference for Pure and Applied Sciences*.
- [20] Ali, I., Wani, W. A., & Saleem, K. (2013). Empirical formulae to molecular structures of metal complexes by molar conductance. *Synthesis and Reactivity in Inorganic, Metal-Organic, and Nano-Metal Chemistry*, 43(9), 1162-1170.
- [21] Saleh, H. A., Rahman, A. S. A. K. A., & Al-Jeboori, M. J. (2021). Synthesis, structural characterisation, and biological evaluation of new semicarbazone metal complexes derived from Mannich-base. *Biochemical and Cellular Archives*, 21(1), 159–168.
- [22] Al-Jeboori, M. J., Numan, A. T., & Ahmed, D. J. (2017). Synthesis and characterisation of novel cobalt (II), copper (II), and mercury (II) complexes of poly vinyl urethanised oxime. *Ibn AL-Haitham Journal for Pure and Applied Science*, 21(2), 89-101.
- [23] Ismail, A. A., & Lateef, S. M. (2023). Synthesis of novel complexes of VO (II), Mn (II), Fe (II), Co (II), Ni (II), Cu (II), and Pt (IV) derived from Schiff's base of pyridoxal and 2-amino-4-nitrophenol and study of their biological activities. *Ibn AL-Haitham Journal for Pure and Applied Science*, 36(2), 259–275.
- [24] Al-Jeboori, M. J., Ameer, A. A., & Aboud, N. A. (2004). Novel pentadentate ligand of $\text{N}_3 \text{S}_2$ donor atoms and its complexes with (Ni^{2+} , Co^{2+} , Cu^{2+} , Fe^{2+} , Hg^{2+} , Ag^+ , and Re^{5+}). *Ibn Al-Haitham Journal for Pure and Applied Science*, 17(3), 80-97.
- [25] Shen, Z., Li, Q., Shi, S., Zang, G., Lv, W., & Zhao, Q. (2024). Studies on synthesis, optical and magnetic properties of Zn, Mn, Co, and Ni complexes of biphenylenedicarboxylic acid ligands. *Journal of Molecular Structure*, 1295, 136661.
- [26] Chouhan, O. P., & Jacob, G. (2014). FTIR, UV-Vis, magnetic, mass spectral and XRD studies of Ni (II) complex with pioglitazone: An oral antidiabetic drug. *Oriental Journal of Chemistry*, 30(4), 1501–1507.
- [27] Zayed, E. M., Zayed, M. A., Hindy, A. M. M., & Mohamed, G. G. (2018). Coordination behaviour and biological activity studies involving theoretical docking of bis- Schiff base ligand and some of its transition metal complexes. *Applied Organometallic Chemistry*, 32(12), e4603.
- [28] Miessler, G. L., Fischer, P. J., & Tarr, D. A. (2013). *Inorganic Chemistry* (5th ed.). Pearson. ISBN: 9780321811059.

[29] Dalal, M. (2017). *A Textbook of Inorganic Chemistry*
– Volume 1. Dalal Institute. ISBN: 9789386202973.

تحضير وتشخيص وتقييم الفعالية المضادة للميكروبات لليكند جديد نوع ثنائي(سيميكاربازون) ومركباته التناسقية

محمد عبد الكريم حميد¹ ، محمد جابر الجبوري^{2*}

المديرية العامة لتربية الانبار، مديرية تربية هيت، الانبار، العراق¹
قسم الكيمياء، كلية التربية للعلوم الصرفة (ابن الهيثم)، جامعة بغداد، بغداد، العراق²

الخلاصة:

تم تصميم هذه الدراسة لتحضير ليكاند جديد متعدد الأسنان من نوع ثنائي السيميكاربازون، (H_2L)، ودراسة مركباته التناسقية ذات الخصائص البارامغناطيسية مع الفلزات الانتقالية ثنائية التكافؤ (أيونات Cu, Mn, Fe, Co, Ni). يركز هذا العمل على تشخيص كل من الليكاند (H_2L) ومركباته التناسقية باستخدام الخصائص الفيزيائية والكيميائية، وتقييم نشاطها المضاد للميكروبات. تم تحضير الليكاند H_2L من بخطوتين وكما يلي: أولاً تم تحضير المادة الأولية (ثنائي الالدهايد) L بخطوتين ثم تم مفاعله مع السيميكاربازيد بنسبة مولية 1:2. تم عزل مجموعة من المركبات التناسقية البارامغناطيسية الأحادية النوات من خلال تفاعل H_2L مع كلوريدات المعادن ($Co(II)$, $Ni(II)$, $Cu(II)$, $Mn(II)$, $Fe(II)$) بنسبة مولية 1:1. تم التحقق من تحضير الليكاند H_2L ومركباته التناسقية ذو البنية الرباعية مع ال ($Ni(II)$)، والمركبات ذات البنية السداسية مع أيونات المعادن الأخرى باستخدام تقنيات تحليلية وطيفية متنوعة، بما في ذلك أطياف ال FT-IR، وأطياف ال UV-Vis، وقياس طيف الكتلة، وأطياف الرنين النووي المغناطيسي (بروتون وكاربون-13) والتحليل الدقيق للعناصر (بما في ذلك محتوى الفلز والكوريد)، وقياسات الحساسية المغناطيسية للمعقدات التناسقية، وقياسات التوصيلية المولارية. بالإضافة إلى ذلك، تم دراسة التحلل الحراري باستخدام ال TGA و DTA لليكاند H_2L وبعض المعقدات. تم تقييم النشاط المضاد للميكروبات لليكاند H_2L ومركباته التناسقية ضد مجموعة واسعة من الأنواع البكتيرية والفطرية. أظهرت المركبات التناسقية نشاطاً مضاداً للميكروبات أعلى مقارنةً بالليكاند H_2L الحر. ومن الجدير بالذكر أن مركبات ($Ni(II)$) و ($Cu(II)$) أظهرت أعلى نشاط ضد السلالات البكتيرية، مع منطقة تثبيط أكبر من تلك الخاصة بالدواء المرجعي أموكسيسيلين. بالإضافة إلى ذلك، أظهرت مركبات ($Co(II)$) و ($Cu(II)$) تعزيزاً كبيراً في مناطق التثبيط ضد فطر *Candida albicans* مقارنةً بالدواء التجاري مترونيدازول.

الكلمات المفتاحية: ليكند ثنائي(سيميكاربازون)، مركبات بارامغناطيسية، التحضير والتشخيص، الاستقرار الحراري، التقييم المضاد للميكروبات